

AUTOMATIC DETECTION OF LUSATIAN CULTURE FORTIFIED SETTLEMENT BASED ON DATA FROM AIRBORNE LASER SCANNING

Artur ŁABUZ¹, Natalia BOROWIEC^{2,*}, Urszula MARMOL²

¹ GEOXY Sp.z o.o., ul. Miedziana 17Krakow, Poland

² AGH University of Science and Technology, Faculty of Geo-Data Science, Geodesy and Environmental Engineering, Krakow, Poland

Abstract

During the first decade of the 21st century, airborne laser scanning became the subject of research for many works in the field of archaeology, which considered the impact and utility of this remote sensing method in archaeological research and focused on its applicability. Today, in addition to other methods used in archaeological work, aerial scanning helps archaeologists understand historical communities and document their activities based on material remains that have survived to this day. Very importantly, research can also take place in forest areas because of the ability of airborne laser scanning to penetrate the forest cover and record the topography of the area. This paper examines the problem of identifying archaeological objects – Grodzisko (fortified settlement), located in Poland, using data from airborne aerial scanning. Various methods of advanced object analysis were presented, i.e., SVF, Slope, TPI and TRI. The acquired images made it possible to carry out identification of remnants of human activity in the past. It was decided to combine the resulting images obtained from the various analyses and perform automatic detection of the fortified settlement. Documentation from previous archaeological investigations was used to verify the results. The accuracy was assessed based on the confusion matrix, where the correctness of the automatic detection of the fortified settlement was at the level of 93% agreement.

Keywords: History; Detection; Archeology; Fortified settlement; LiDAR; DTM analyzes

Introduction

Airborne laser scanning has become an increasingly popular tool in the archaeology area in recent decades [1–3]. LiDAR (Light Detection and Ranging) is an active technique for remotely gathering information about objects and phenomena. The obtained point cloud allows the reconstruction of Digital Terrain Model (DTM) and Digital Surface Model (DSM) [4]. A great advantage of acquisition of point clouds by LiDAR technology is registration of information of areas difficult to access, especially wooded areas covered with high, dense vegetation, where it is not possible to perform traditional height measurements. The method of airborne laser scanning makes it possible to locate difficult to access objects with a specific terrain form, i.e., embankments, fortified settlements, barrows. In archaeology, because of the ability to penetrate the laser pulse, LiDAR technology not only allows to confirm previous discoveries and accurately

* Corresponding author: nboro@agh.edu

measure them, but also to find new objects, the location of which researchers have so far had only speculations [5–8].

The present study is concerned with the analysis of an Early Medieval castle on the Grodzisko hill in Poznachowice Dolne in the Malopolska province of Poland. Traditional archaeological research was conducted at the site during 1950-1990. Currently, the site is located on a mountain track, is covered with tall trees and is very difficult to identify.

In this work, data from airborne laser scanning was used due to the quality and high spatial resolution which makes possible to capture the subtle differences in the topographic terrain. The resulting models are an ideal source of information for verifying and refining the results of archaeological studies previously conducted.

The research was conducted on data collected from the ISOK (IT system for protecting the country) project in Poland [9]. ISOK is a project aimed at creating a system to protect the Poland from extraordinary threats, especially floods. Airborne laser scanning data has been available to the public since 2020.

Review of the literature

One of the most spectacular examples of the effective use of laser scanning in archaeology was the discovery of Caracol, an ancient Mayan city in what is now Belize in 2010 [10]. Field work in the area took 25 years to survey only 23 square kilometers of the complex, so it was decided to use laser scanning. The flight was carried out in the dry season, when vegetation was less abundant although in principle tree cover is not an obstacle to taking measurements, such dense vegetation as is found in tropical forests would have distorted the survey results. It took only four days of flights to discover a huge urban area (buildings, roads, causeways, cultivated terraces) in an area of 200 square kilometers, which was inhabited by more than 115.000 people in its glory years. The Caracol example is the first-time laser scanning surveys have been performed on such a large scale. The survey was also groundbreaking in the sense that until now individual archaeological sites had been studied rather than considering the scale at which ancient Maya cities were built.

Laser scanning has also played a significant role in the discovery of Roman military sites in northwestern Spain [11]. The study proposed various methods for distinguishing microtopography from simple shading techniques to more complex calculations such as combinations of slope and DTM shading, Principal Components Analysis, Sky View Factor, Local Relief Models, Openness.

In order to document archaeological sites and obtain their 3D digital models, several methods are possible, such as the combination of terrestrial recording and photogrammetric aerial methods, using unmanned aerial vehicles (UAVs). Images from the UAV were used for three-dimensional reconstruction of several archaeological sites in Tulcea County [12]. A photogrammetric methodology was applied to produce a scale 3D model of “Arutela Roman Castrum” in a digital environment [13]. A complex product is created, with complementary geometry and texture.

So far in Poland, there have also been some interesting examples of the use of lidar data in archaeology. The research became significantly more activated when the aerial scanning of the country was carried out in 2011-2014 as part of the ISOK project. There is no question that airborne laser scanning is an essential tool in the search for new archaeological sites, especially in large, forested areas, of which the ISOK project covered tens of thousands of square kilometers of Polish territory.

One of the interesting discoveries is a settlement in the Wdecki Landscape Park in Kujawsko-Pomorskie Province. In 2018, archaeologists found signs of a settlement in a dense forest. Using airborne laser scanning data, the spatial arrangement of the settlement along with homesteads, fields, baulks, and roads was extracted. The discovery was unique in Europe, and the settlement was called the second Biskupin by the media [14].

Another example of the use of airborne laser scanning data for modern history research was an attempt to reconstruct World War II trenches in the Makowski Beskid. Here, field measurements were also taken using GPS [15]. Both methods used complemented each other, as the field survey prevented incorrect interpretation of the image generated from the LiDAR data. As a result of the methods' integration, it was possible to identify a line of trenches, 16.160 meters long, in a vast and inaccessible area with significant forest cover. The method made it possible to distinguish the defense line from other linear objects, such as forest ducts, for example.

Different survey using laser scanning technology in Poland was conducted on the Grojec hill on the border of the Żywiec and Radziechowy-Wieprz communities. The hill had been inhabited since ancient times, and in the Early Middle Ages there was a robbers' castle on its peak. It was probably destroyed in 1462. Based on the raster generated from the lidar data, it was possible to indicate the exact boundaries of the parcels, even though agricultural activities have not been carried out there for many years. And there have also been changes on the hill due to modern human activity the construction of a ski slope and the Amphitheater under Grojec [16].

Another example documenting the fortresses of the medieval Wolek castle in the Beskid Mały village of Kobiernice in southern Poland is the researched in other publication [17].

One study [18] presents the morphometric parameters of craters and the reconstruction of their emergence and transformation processes, which are stored in landform morphology. The usefulness and accuracy of digital elevation models and shaded relief rasters was tested for different resolutions in the analyses of craters occurring in a variety of environmental conditions.

The above examples show that not only in the world, but also in Poland, research in the field of archaeology is carried out using LiDAR. This method works well both in identifying barrows or fortified settlements, as well as in systematizing and expanding knowledge of recent history.

Data and study area

The study was carried out at the Grodzisko located in the Ciecień hill range, in Poznachowice Górne, Subcarpathia. There are two archaeological sites on top of Grodzisko one of them is an Early Medieval castle, while the other is the so-called "Monastery", located on the eastern part of the hill.

The study used open access LiDAR data from the National Geoportal - Poland [19]. These data are from high altitude airborne laser scanning. The point cloud was downloaded in LAZ format for the complete section numbered M-34-77-C-b-3-1-4, coordinate system PL-2000, PL-KRON86-NH. The point density in the study area is 12 points per square meter. Based on the dense point cloud, a 0.5m Digital Terrain Model was created (Fig. 1).

The current embankments of the settlement as well as the top marker and board memorializing the partisan units stationed at the settlement during World War II are shown in Figure 2.

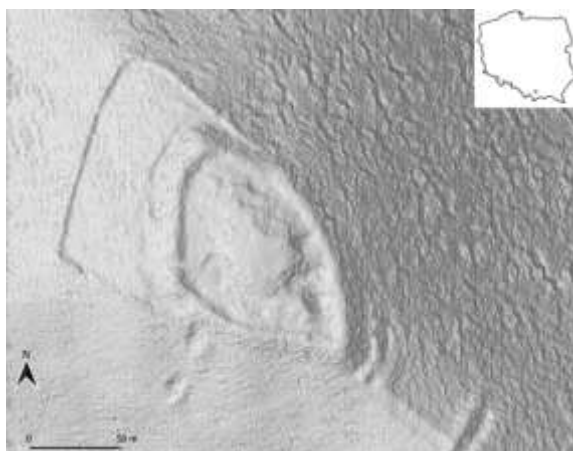


Fig. 1. Study site location in Poland and enlarge of the analyzed zone, where the LiDAR data was used to build the Digital Terrain Model



Fig. 2. Current state: a) Grodzisko embankments; b) Top marker and boards memorializing partisan units stationed on Grodzisko during World War II

Previous archaeological research at Grodzisko

The first preliminary descriptions of Grodzisko as an archaeological site appeared as early as the second half of the 19th century. However, this was only a brief description of the layout of the embankments and a statement that it was a "colossal construction site" [20].

The author of another description of Grodzisko was, in 1902, Stanisław Zakrzewski, who investigated the beginnings of a Cistercian monastery in nearby Szczyrzyc and the development of settlements in the Stradomka and Krzyworzeka basins from the 13th to the 14th centuries. He came up with a hypothesis, which, however, was not confirmed in the scientific literature, that Grodzisko was the seat of a castellan in the Early Middle Ages [21].

In the following years, researchers visited the site several times more and described it in the scientific literature, while the first archaeological excavations at Grodzisko were not carried out until the 1950s. In 1952, work on the hill was conducted by Andrzej Źaki, while in 1955-1956 by Gabriel Leńczyk. During the excavations, the central part of the castle, the space between the embankments and the defensive fortifications were examined. The work uncovered cultural

objects and movable relics from different chronological periods. Most were found relics of the Lusatian culture from the Halstatt period and La Tène pottery of the Celtic culture. This does not mean that Early Medieval remains, to which the castle was dated, were not found in several excavations, being found many vessel fragments from this period [21].

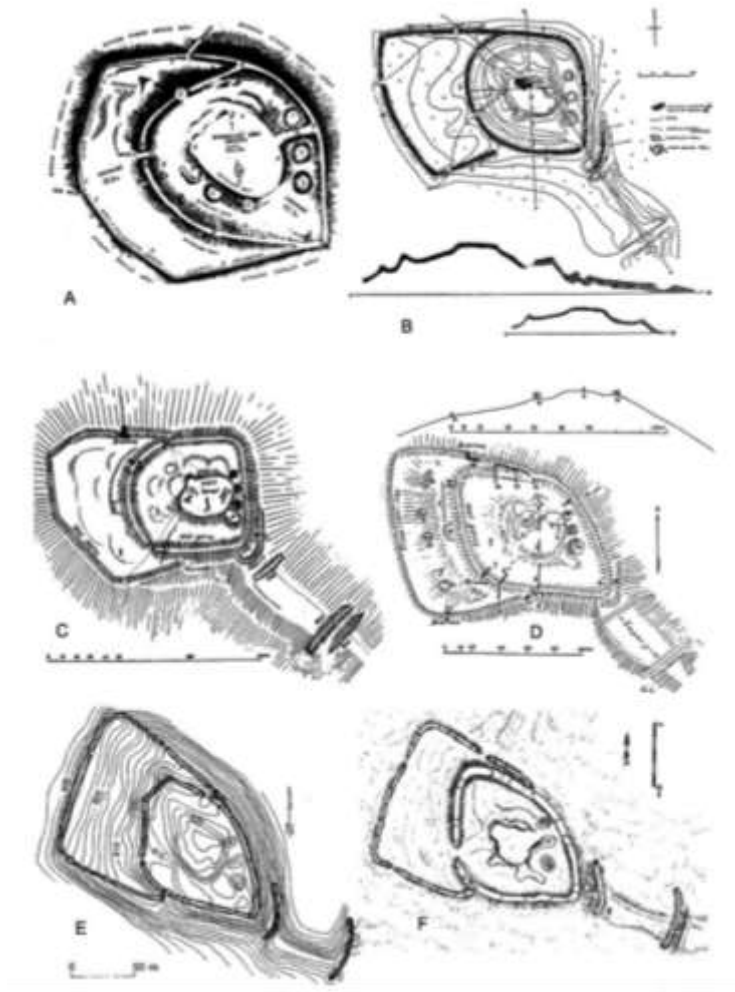


Fig. 3. Poznachowice Górne, Myslenice district, state. 1 "Grodzisko".

Plan of the fortified settlement according to: a – W. Demetrykiewicz and M. Wawrzyński; b – A. Żaki; c, d – G. Leńczyk; e – A. Jodłowski; f – G. Mądrycki, source: [22]

On the basis of the studies carried out, Andrzej Żaki suggested a hypothesis that as many as three consecutive fortified settlements erected by Lusatian-Pomeranian, Celtic and early Polish peoples functioned in succession at the site of the excavations. Gabriel Lencyk, on the other hand, indicated that the embankments were built in the earlier phase of the Early Middle Ages. Despite the research, it has still not been possible to determine the nature of settlement on the hill in earlier periods, as well as the exact dating of the last of the embankments. In 1979-1980, another archaeological survey was conducted, this time under the direction of Antoni Jodłowski, on behalf of the Cracow Saltworks Museum in Wieliczka. They confirmed Żaki's hypothesis of three consecutive settlements, representing the periods: Halstattian and possibly Early Latin, Late Latin and Early Roman, and the late stage of the Early Middle Ages. The last of the fortified

settlements was probably built in the early 12th century and was surrounded by a ring-shaped embankment in a timber, stone and earth structure. On the other hand, it was adjoined to the west by a subgarden surrounded by a stone wall. The differences in the construction of these two parts may suggest different times of construction. The end of the castle's functioning in the mid-13th century and the fact that it burned down is evidenced by burnt stones and clay along the entire length of the embankments. The last of the archaeological investigations carried out at the site took place in 1990-1991. Figure 3 shows a plan of the settlement developed by archaeologists in the following years.

The final Grodzisko plan has been presented by J. Poleski [22] on figure 4.

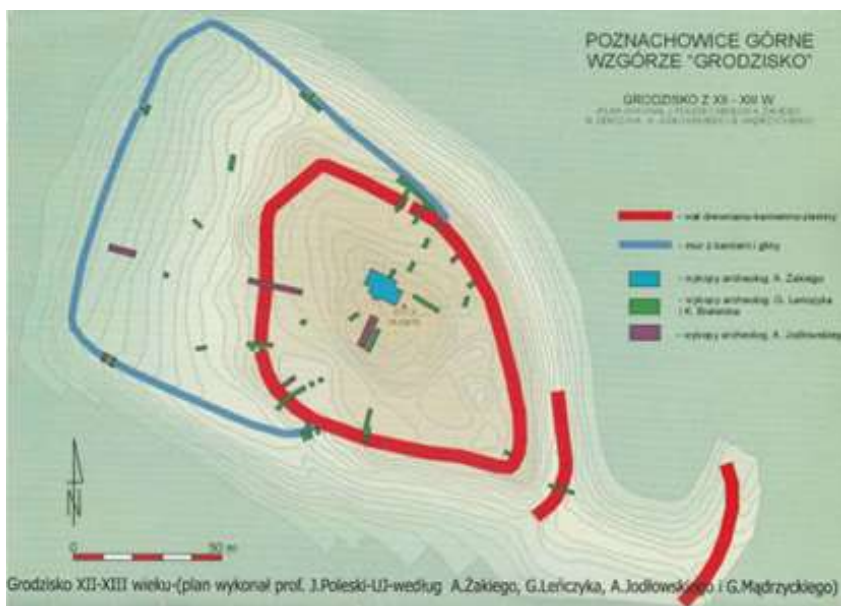


Fig. 4. Plan of the fortified settlement with archaeological excavation indicated [22]

Comparative analysis of LiDAR data with archaeological research results from the 1980s

Archaeological description of the fortified settlement

The castle on the Grodzisko hill in Poznachowice Górne was precisely measured in 1983 during archaeological research conducted under the direction of Professor Antoni Jodłowski [21]. According to these measurements, the main part had the shape of an irregular oval with dimensions of 128 by 80 meters. At that time, the width of the embankment was 10 meters, and its height reached up to 2 meters on the inner side, and up to 5 meters on the outer side.

Among the castle, a clearly distinguishable top plane was also measured in the field, which, like the castle, was shaped like an oval with dimensions of 42 by 30 meters. In addition, there was an ancillary settlement adjacent to the castle to the west, in the shape of a relatively regular quadrangle measuring 122 by 50 meters. A bracken shaped embankment built of local stone connected to the upper embankment in the northern and southern sections. The width, as measured, ranged from 2.5 to 3 meters, and the height was 1.5 meters.

On the south-eastern side next to the fortress were two more transverse embankments with ditches. One of them was located at 12 meters from the upper embankment of the fortress. It was measured to be 43 meters long, 3 meters wide and 1 meter high. The second barrier embankment was erected 55 meters from the corner of the majdan. It was 56 meters long, while its width was similar to that of the first embankment.

Metric analysis of the object based on LiDAR data

Based on the obtained point cloud, DTM with a grid size of 0.5m was generated. In the first stage of analysis, measurements of the object were carried out. The following results were obtained on Figure 5:

- The castle is 130 metres by 80 metres, and measurements of the thickness of the upper embankment in different positions give results of 10 to 15m. Its height reaches up to 5.8m from the outside, 2m inside.
- The top plane dimensions are 41m by 30m.
- The ancillary settlement is similar to a quadrangle measuring 119m by 40-48m, with a embankment width of 2.5 to 3m and a height of 1.5m.
- The first transverse embankment is located 12m from the south-east corner of the castle, and is 45m long, 4m wide and 1m high.
- The second transverse embankment is 56m from the south-east corner of the castle, 3m wide and 1m high.

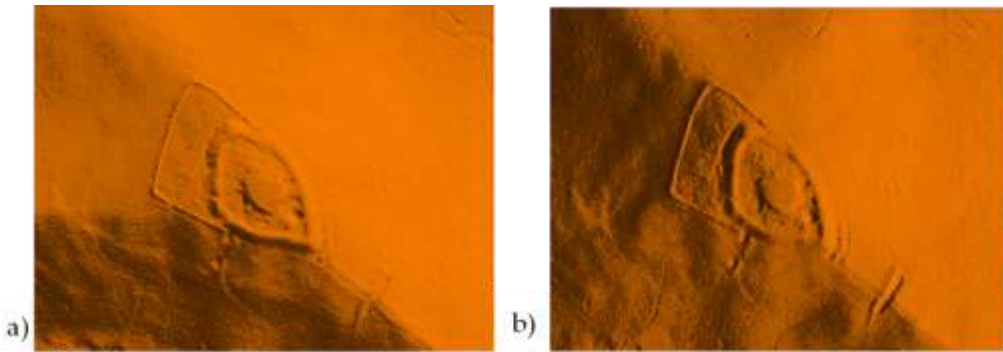


Fig. 5. Object at different sun azimuth and sun angle settings
 a) sun azimuth = 45°, sun angle = 25°, b) sun azimuth = 90°, sun angle = 15°

The analysis of the LiDAR results confirms that the data are consistent with field measurements and that the differences between them are very small. This demonstrates that the use of this technology can facilitate or replace traditional and tedious field measurements.

Advanced object analysis based on LiDAR data

Based on the DTM it is possible to make a preliminary determination of local changes of probable anthropogenic origin. Visual interpretation of the DTM requires the ability to recognize knowledge-based patterns and the ability to identify and classify complex landforms on the basis of the material on the study site, experience and previous archaeological knowledge. Once possible man-made features are detected on the DTM, analyses of the site are made on its derived products.

Of the different advanced DTM visualization algorithms commonly operating in world archaeology, attention should be drawn to Sky View Factor analysis, which recalculates the extent of the hemisphere accessible from a given location on the model under analysis [23]. SVF for a point on a grid is calculated from the formula below:

$$SVF = \int_{\theta=0}^{2\pi} \cos^2(\beta(R, \theta))d\theta \quad (1)$$

where: β is an angle from the center point to the maximum obstacle height at a maximum distance equal to the constant search radius (R). When integrating this formula over all directions ($d\theta$) from 0 to 2π , the SVF for the full hemisphere is obtained [21].

The SVF causes locally flat terrain, ridges and earth structures that receive more light to stand out and appear bright (SVF values close to 1 almost the entire hemisphere above the pixel is visible), while depressions (ditches, moats, pits) are dark because they receive less light (SVF values close to 0). The raster resulting from the analysis is shown in Figure 6.

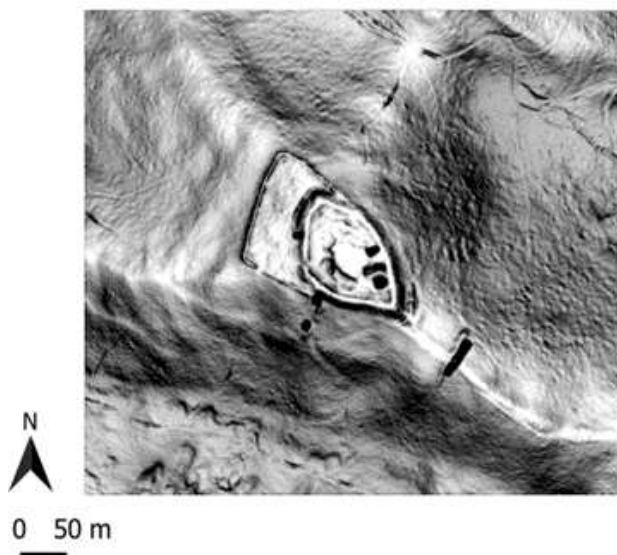


Fig. 6. Sky View Factor visualization

Considering the recommendations for the use of LiDAR data visualisation techniques in other archaeological research work, the value of the maximum horizon search radius was set at 10m. The choice of the value of this parameter is related to its impact on the SVF result the larger the radius, the more generalised the results. In contrast, a small search radius can be used to visualise and classify local morphological forms [25].

As a result of the interpretation of the obtained data, it was found that the embankments of the fortress and the stone and clay wall on the SVF model created (Fig. 6) are clearly visible. In the western part of the analysed area, a much darker contour is noticeable on the right side of the stone wall, which indicates the existing depressions around the wall. The same phenomenon can be observed in the north-western part of the enclosure, to the left side. The top of the fortress, on the other hand, takes on a light colour, which indicates that the embankments have degraded and flattened due to the passing of time and exogenic processes and human activity. The top, and at the same time the inner part of the fortress, is very light-coloured, which may indicate the presence of buildings. In the interior of the fortress, on the eastern side, dark areas are also visible, reflecting earlier excavations at these sites.

In the next step of the study, the slope map (Fig. 7) was determined based on the formula:

$$\alpha = \arctan \sqrt{\left(\frac{dz}{dx}\right)^2 + \left(\frac{dz}{dy}\right)^2} \quad (2)$$

where: dz/dx – slope in the x-direction, dz/dy – slope in the y-direction.

Interpretation of slope maps is problematic without additional information. However, it can be seen in the figure that dark pixel values indicate steep slopes, while flat areas are represented by bright pixel values. Therefore, the visible light linear elements reflect the flattening of the embankments, while the dark elements are the locations of the foothills of the embankments.

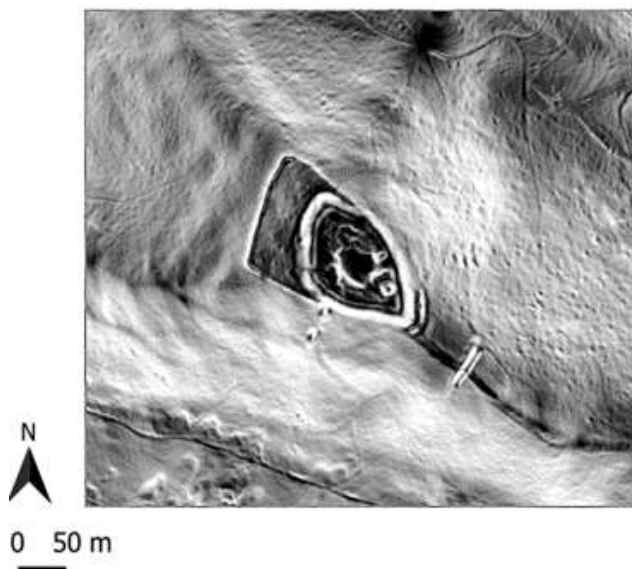


Fig. 7. Slope map

Another important parameter used in archaeology is the topographic position index (TPI), proposed in 2001 by A. Weiss [26]. This is a method of land classification in which the height of each point is calculated in relation to its neighbourhood [27]. TPI is calculated by subtracting the average height of neighbouring pixels from the height of the central cell:

$$TPI = z_0 - \frac{\sum_{1-n} z_n}{n} \quad (3)$$

where: z_0 - central cell height, z_n - neighbouring cell height and n – width of moving window.

If a point is higher than its surroundings, the index will be positive, for example on ridges and tops of hills, while the value will be negative for depressed features such as valleys. In the created visualisation (Fig. 8), the grey colours represent values close to or equal to 0 and these sites represent areas that are flat or have a constant slope. On the other hand, very bright colours indicate positive TPI values, i.e., the occurrence of sites much higher than their surroundings. On the visible raster, the locations of the embankments and even the exact course of their edges are clearly visible.

Another tool is the terrain roughness index (TRI), which is a measure of topographic heterogeneity, the variety of relief [25]. This method calculates for each pixel the average vertical difference with its eight neighbours. The terrain heterogeneity index is determined for each raster cell by calculating the square root of the sum of the squared height differences between the central pixel and its neighbours in a specified neighbourhood:

$$TRI = \left[\frac{1}{N^2-1} \sum_{k=1}^{N^2} (z_0 - z_k)^2 \right]^{\frac{1}{2}} \quad (4)$$

where: z_0 - central cell height, z_k - neighbouring cell height and N – width of moving window.

Figure 9 shows the result of the TRI visualisation for the study area. The closer the values are to 0 (black colour), the less variation in the terrain - the area is flat or has a uniform slope. The brighter the colour, the more varied the relief is, indicating that there are differences between the heights of neighbouring pixels in relation to the central pixel. The resulting image clearly shows the white linear elements that reflect the locations of the embankments. The outline of the whole fortress is visible very accurately. The areas inside the embankment are of a slight slope.

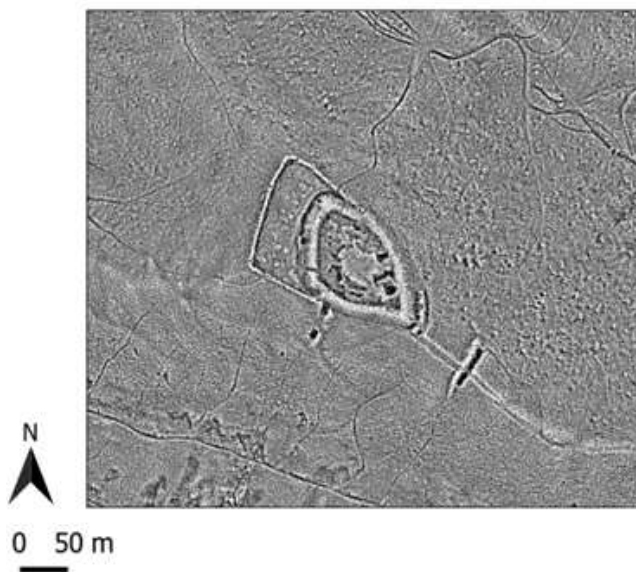


Fig. 8. TPI visualization

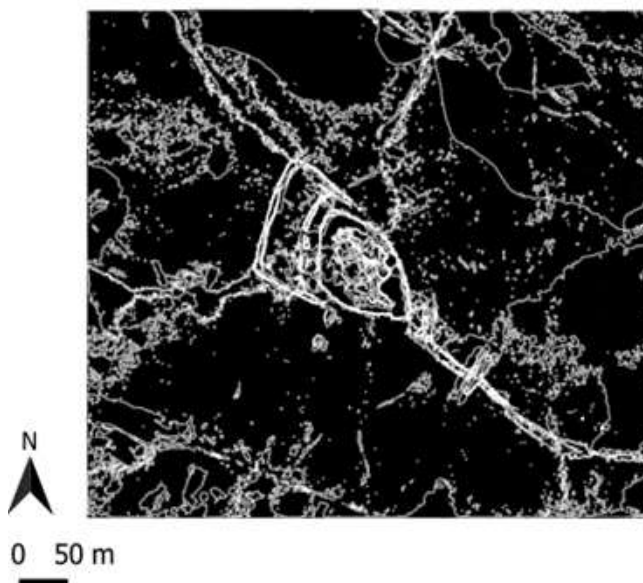


Fig. 9. TRI visualization

Automatic detection of fortified settlement

Before proceeding the obtained results were filtered from noise using median filters and closing operators. The next stage of the fortified settlement detection was to reclassify the corrected images: Sky View Factor, slope map, TPI and TRI. The results obtained are presented in Figure 10.

The above obtained images were compared with data acquired by traditional archaeological measurements. Visual and accuracy assessments were made. Comparisons were made between archaeological maps from 80's, which were produced by traditional methods, and the results of automatic detection carried out on LiDAR data (i.e., images SVF, slope, TPI, TRI). In the first step, an affine transformation was performed to fit the archival archaeological map

into the digital maps and georeferenced them. Then digitalization of each element on the archival archaeological map was carried out manually. The next steps involved a pixel-by-pixel comparison (50cm resolution) between the archaeological map and the results obtained by automatic detection. This approach makes it possible to build confusion matrix which count the number of pixels of the four possible outcomes: TP - true positive (successful detections of fortified settlement), TN - true negative (correct detection that the fortified settlement does not exist in this location), FP - false positive (erroneous detections of fortified settlement) and FN - false negative (undetected fortified settlement).

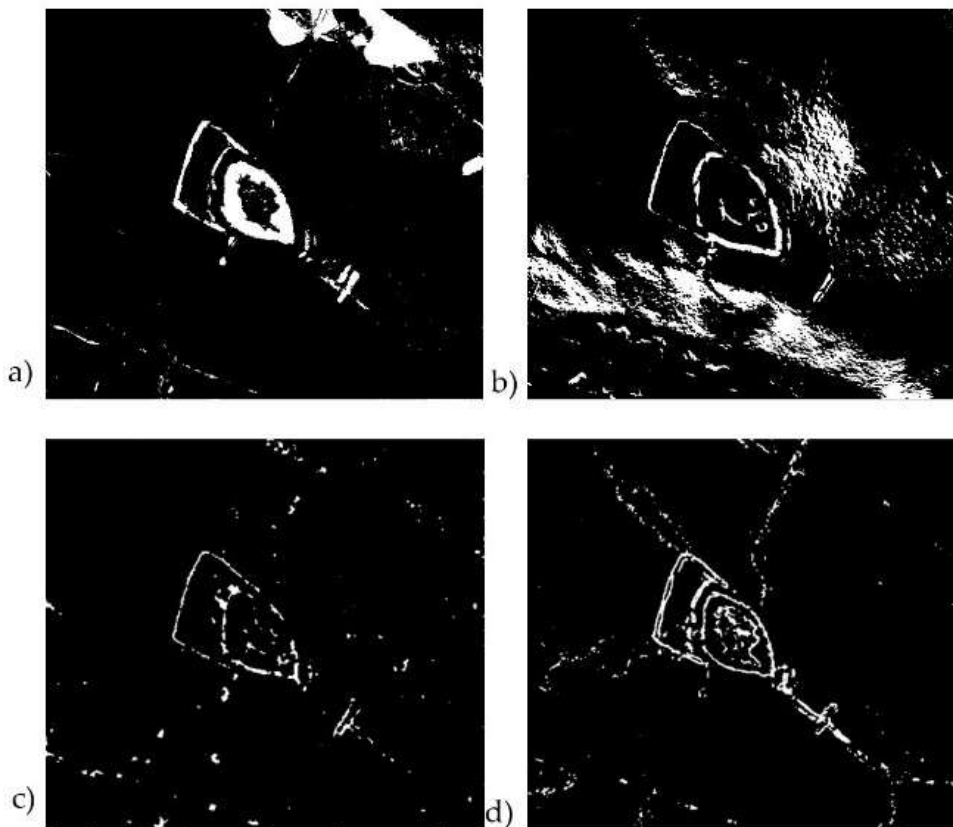


Fig. 10. Results of image reclassification: a) Sky View Factor; b) slope map; c) TPI; d) TRI

The confusion matrix enables the calculation of common capacity index of the automatic detection process using LiDAR data [28–30]. The following parameters were calculated:

- True positive rate (TPR) is the probability that the detection result is positive when the fortified settlement is present:

$$TPR = \frac{TP}{TP+FN} \quad (5)$$

- Positive predictive value (PPV) is the probability that the fortified settlement is present when the detection result is positive:

$$PPV = \frac{TP}{TP+FP} \quad (6)$$

- Negative predictive value (NPV) is the probability that the fortified settlement is not present when the detection result is negative:

$$NPV = \frac{TN}{TN+FN} \quad (7)$$

- True negative rate (TNR) is the probability that the detection result is negative when the fortified settlement is not present:

$$TNR = \frac{TN}{TN+FP} \quad (8)$$

Results and discussion

The quality of the automatic detection process is visually verified at the scale of each pixel. The figure below shows what part was detected automatically and overlaps with the old archaeological map (Fig. 11).

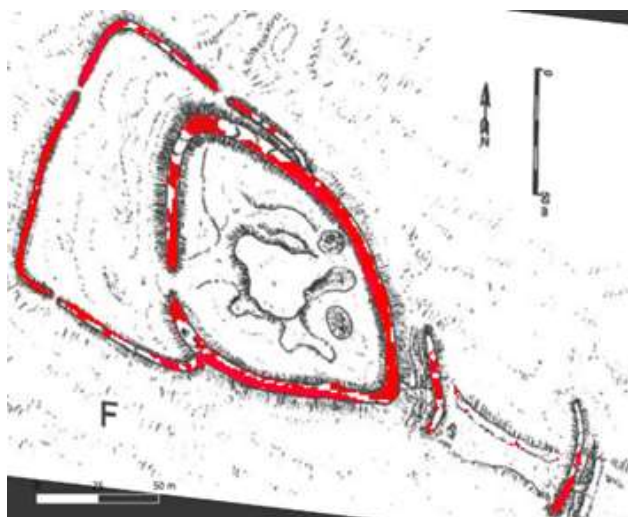


Fig. 11. Red pixels – automated detected fortified settlement. Results on the background of the old archaeological map

Accuracy indicates what proportion of pixels, out of all those classified, were classified correctly as a fortified settlement. In this study automatic detection overlapped with archival maps at 93%. While, in the present study, reliability was assessed as individual elements of the fortified settlement. Thus, the wood-stone-soil dike was correctly detected at 89%. The north-western section of the dike was the least detected. Despite the lack of accurate detection, the outline of the embankment is very visible. A narrower but higher stone wall was automatically detected at the 96% level. In addition, there are two transecting dikes on the southeast side, where the first was detected at 92%, while the second was detected at 91%.

The evaluation of the results on the scale of each pixel is presented in the table below. The Table 1 gives the values of the quality indicators computed, in terms of number of pixels.

Table 1. Quality indicators at the pixel scale

True Positive	True Negative	False Positive	False Negative
2693	22372	328	635
TPR	PPV	NPV	TNR
0,891	0,809	0,986	0,972

The TPR and TNR parameters receive respectively values of 0.891 and 0.972, which shows that automatic detection and localization has been performed at a high level. The positive predictive value (PPV) of 0.809 and the negative predictive value (NPV) of 0.986 reveals that

dike detection capability is possible with more false detections (false positive) than undetected features (false negative). The false positive pixel count of 635 indicates that the pixels were detected as dikes, when in fact they are not. On the other hand, the number of undetected pixels (false negative) is relatively small because the total is 328. Most erroneous detections are in close areas, which mainly represent fragments of the surroundings detected dikes. The other erroneous detections are fragments of present-day mountain trails.

The results are satisfactory considering that the point of cloud is obtained in a fast way, and the density of points in the area averaged is 12 pts/m², which made it possible to generate rasters with a resolution of 0.5m. A higher resolution would allow more detail to be acquired. An alternative could be LiDAR but obtained from a UAV height.

It is also important to specify that the analyzes carried out were in a mountainous area and now is covered with high trees. Viewing only the orthophotos, the fortified settlement is not visible at all (Fig.12).



Fig. 12. Automated detected fortified settlement (red pixels) on the background of the orthophotomap

An important aspect in this research is that information on archaeological data was obtained automatically. Thus, LiDAR can be a new tool to support automatic detection of archaeological sites. The aim is not to build full automation of the detection process of various archaeological objects, but to promote close cooperation between archaeologists and photogrammetrists. The effectiveness of automatic detection largely depends on the current terrain. Thus, it is necessary to correctly select tools that will accurately identify archaeological objects, which requires experience and correct interpretation of the results.

Conclusions

The literature review and the completed analysis of the fortified settlement in Poznachowice Górne confirm the great usefulness of laser scanning data for detecting and developing archaeological sites. These allow the discovery of previously unknown or only surmised locations. The analysis of data obtained from LiDAR in combination with field surveys allows to obtain very good results, and both methods complement each other very well.

The identification of archaeological sites depends on the method used to visualize the model derived from laser scanning. For simple analyses using shading, the visibility of potential objects is greatly affected by the direction and height of the incident rays. Therefore, a very good way to improve visibility is to use more complex presentation methods. The study shows the benefits of using methods such as Sky View Factor, Slope Map, Topographic Position Index and Terrain Ruggedness Index.

As a result of the research, the best interpretative results were achieved by assembling the results from different methods together. Then the identification of the entire fortified settlement is the best, and which was confirmed by comparing the results with archival archaeological maps. However, experience indicates that for automatic detection it is not possible to choose a single method that will always give optimal results. A lot depends on the type of archaeological structure. In this case, linear elements were researched, while it would be an interesting experience to check point objects. In addition, the interpretation of the results is important. So, in summary, the effectiveness of the algorithm for recognizing different archaeological patterns is strongly dependent on the current terrain. This means that it is necessary to correctly select tools and accurately interpret the results.

In conclusion, although laser scanning gives very good results in detecting archaeological sites and verifying previous research, it is not possible for us to distinguish the stages of archaeological site formation, but only the last stage of activity at a given site. Which makes it still necessary to conduct additional archaeological research in the field. This is why cooperation between archaeologists and photogrammetrists is so important.

Acknowledgments

The authors thank the editor and anonymous reviewers for their helpful comments and valuable suggestions.

Data Availability Statement: The data presented in this study (.las files) are available in ISOK project - <https://isok.gov.pl/index.html> - accessed on 20 July 2022.

The article was prepared under the research subvention of the AGH University of Science and Technology No. 16.16.150.545 in 2023.

References

- [1] B. Štular, S. Eichert, E. Lozić, *Airborne LiDAR Point Cloud Processing for Archaeology. Pipeline and QGIS Toolbox*, **Remote Sensing**, **13**(16), 2021, Article Number: 3225, <https://doi.org/10.3390/rs13163225>.
- [2] R.H. Bewley, S.P. Crutchley, C.A. Shell, *New light on an ancient landscape: lidar survey in the Stonehenge World Heritage Site*, **Antiquity**, **79**(305), 2005, pp. 636 - 647, <https://doi.org/10.1017/S0003598X00114577>.
- [3] G. Mussumeci, O. Palio, M. Mangiameli, I. Berganzo-Besga, H.A. Orengo, J. Canela, M.C. Belarte, *Potential of Multitemporal Lidar for the Detection of Subtle Archaeological Features under Perennial Dense Forest*, **Land**, **11**(11), 2022, Article Number: 1964, <https://doi.org/10.3390/land11111964>.
- [4] S.K. Będkowski, M. Brach, K. Stereńczak, *Digital terrain model of forested area based on laser scanning and its accuracy*, **Roczniki Geomatiki**, **6**(8), 2008, pp. 49-55.
- [5] B.J. Devereux, G.S. Amable, P. Crow, A.D. Cliff, *The potential of airborne lidar for detection of archaeological features under woodland canopies*, **Antiquity**, **79**(305), 2005, pp. 648-660, <https://doi.org/10.1017/S0003598X00114589>.
- [6] O. Seitsonen, J. Ikäheimo, *Detecting Archaeological Features with Airborne Laser Scanning in the Alpine Tundra of Sápmi, Northern Finland*, **Remote Sensing**, **13**(8), 2021, Article Number: 1599, <https://doi.org/10.3390/rs13081599>.

- [7] E. Rodríguez González, P. Paniego Díaz, S. Celestino Pérez, M. Checa, D.D. Alexakis, *Lost Landscape: A Combination of LiDAR and APSFR Data to Locate and Contextualize Archaeological Sites in River Environments*, **Remote Sensing**, **13**(17), 2021, Article Number: 3506, <https://doi.org/10.3390/rs13173506>.
- [8] M. Niculiță, *Geomorphometric Methods for Burial Mound Recognition and Extraction from High-Resolution LiDAR DEMs*, **Sensors**, **20**(4), 2020, Article Number: 1192, <https://doi.org/10.3390/s20041192>.
- [9] * * *, *Informacyjny System Oslony Kraju - ISOK*, <https://isok.gov.pl/index.html> [access on 17 November 2022].
- [10] A.F. Chase, D.Z. Chase, J.F. Weishampel, J.B. Drake, R.L. Shrestha, K.C. Slatton, J.J. Awe, W.E. Carter, *Airborne LiDAR, archaeology, and the ancient Maya landscape at Caracol, Belize*, **Journal of Archaeological Science**, **38**, 2011, pp. 387-398, <https://doi.org/10.1016/j.jas.2010.09.018>.
- [11] J. Costa-García, A. Blanco, D. González-Álvarez, M. Gago, J. Fonte, R. Blanco-Rotea and V. Martínez, *The Presence of the Roman Army in North-Western Hispania: New Archaeological Data from Ancient Asturias and Galicia*, **Limes XXIII. Proceedings of the 23rd International Congress of Roman Frontier Studies Ingolstadt 2015** (Editors: C.S. Sommer, S. Mastešić), Kommission: Nünnerich-Asmus Verlag-Mainz, 2018, pp. 903-910.
- [12] A.V. Tache, I.C.A. Sandu, O.C. Popescu, A.I. Petrișor, *UAV solutions for the protection and management of cultural heritage. Case Study: Halmyris archaeological site*, **International Journal of Conservation Science**, **9**(4), 2018, pp. 795-804.
- [13] I. Cărlan, B. Dovleac, *Conservation Science 3D Modelling of Arutela Roman Castrum using close-range photogrammetry*, **International Journal of Conservation Science**, **8**(1), 2017, pp. 35-42.
- [14] * * *, *Zabytki archeologiczne w świetle lasera*, *Serwis Akademii Górniczo-Hutniczej*, <https://www.agh.edu.pl/aktualnosci/info/zabytki-archeologiczne-w-swietle-lasera> [access on 17 November 2022].
- [15] P. Franczak, W. Jucha, *Identification of the infrastructure of defence from the period of the second World War in areas of forest by lidar data*, **Zarządzanie Ochroną Przyrody w Lasach** **09**, 2015, pp. 130-142, DOI: 10.5604/20811438.1206163
- [16] W. Jucha, A. Marszałek, *Application of ALS data in interpretation of past and contemporary land use forms using the example of Grojec hill*, **Roczniki Geomatyki**, **14/4**(74), 2016, pp. 465-476.
- [17] N. Słowińska, A. Żyła, N. Borowiec, *Verification of the Wolek Castle Model with the Actual State Using Digital Photogrammetry and Conventional Survey Methods*, **Geomatics and Environmental Engineering**, **17**(1), 2023, pp. 35-55, <https://doi.org/10.7494/geom.2023.17.1.35>.
- [18] J.M. Waga, B. Szypuła, M. Fajer, *Heritage of war: analysis of bomb craters using lidar (Kędzierzyn-Koźle, Poland)*, **International Journal of Conservation Science**, **13**(2), 2022, pp. 593-608.
- [19] * * *, *Geoportal.gov.pl* https://mapy.geoportal.gov.pl/imap/Imgp_2.html?gpm=gp0 (access on 17 November 2022).
- [20] W. Chlebowski, B., Sulimierski, F., Walewski, **Słownik Geograficzny Królestwa Polskiego i Innych Krajów Słowiańskich, Tom II**, Warszawa, 1881.
- [21] A. Jodłowski, *Grodzisko w Poznachowicach Górnych, woj. krakowskie, w świetle wstępnych badań archeologicznych*, **Sprawozdania Archeologiczne**, **35**, 1983, pp. 249-262.
- [22] A. Andrzejewski, J. Sikora, **Grodziska Wczesnośredniowieczne Polski Centralnej. Archeologiczne badania Nieinwazyjne z Lat 2013-2016**, Łódź, 2017.
- [23] Ł. Banaszek, *Lotniczy skaning laserowy w polskiej archeologii. Czy w pełni wykorzystywany jest potencjał prospekcyjny metody?*, **Folia Praehistorica Posnaniensia**, **19**, 2014, pp. 207-251.

- [24] M. Dirksen, R.J. Ronda, N.E. Theeuwes, G.A. Pagani, *Sky view factor calculations and its application in urban heat island studies*, **Urban Climate**, **30**, 2019, Article number: 100498, <https://doi.org/10.1016/j.uclim.2019.100498>.
- [25] K. Zakšek, K. Oštir and Ž. Kokalj, *Sky-View Factor as a Relief Visualization Technique*, **Remote Sensing**, **3**(2), 2011, pp. 398-415, <https://doi.org/10.3390/rs3020398>.
- [26] A.D. Weiss, *Topographic position and landforms analysis*, **Proceedings of the ESRI User Conference, San Diego, CA, USA, 9–13 July 2001**, pp. 227–245. Available online: http://www.jennessent.com/downloads/TPI-poster-TNC_18x22.pdf [accessed on 28 January 2019].
- [27] J. De Reu, J. Bourgeois, M. Bats, A. Zwertvaegher, V. Gelorini, P. De Smedt, W. Chu, M. Antrop, P. De Maeyer, P. Finke, M.V. Meirvenne, J. Verniers, P. Crombé, *Application of the topographic position index to heterogeneous landscapes*, **Geomorphology**, **186**, 2013, pp. 39-49, <https://doi.org/10.1016/j.geomorph.2012.12.015>.
- [28] T. Fawcett, *An introduction to ROC analysis*, **Pattern Recognition Letters**, **27**(8), 2006, 861-874, <https://doi.org/10.1016/j.patrec.2005.10.010>.
- [29] H.G. Lewis, M. Brown, *A generalized confusion matrix for assessing area estimates from remotely sensed data*, **International Journal of Remote Sensing**, **22**(16), 2001, pp. 3223-3235, <https://doi.org/10.1080/01431160152558332>.
- [30] P. Cavalin, L. Oliveira, *Confusion matrix-based building of hierarchical classification*, **Progress in Pattern Recognition, Image Analysis, Computer Vision, and Applications. CIARP 2018. Lecture Notes in Computer Science**, vol. 11401, (Editors: R. Vera-Rodriguez, J. Fierrez, A. Morales) Springer, Cham, 2019, https://doi.org/10.1007/978-3-030-13469-3_32.

Received: August 03, 2022

Accepted: January 14, 2023